J. Physiol. (1981), **317**, *pp.* 129–148
With 11 *text figures*
Printed in Great Britain

IMMOBILIZATION OF MEMBRANE CHARGE IN FROG SKELETAL MUSCLE BY PROLONGED DEPOLARIZATION

BY R. F. RAKOWSKI

From the Department of Physiology and Biophysics, Washington University School of Medicine, St Louis, Missouri 63110, U.S.A.

(*Received 7 January 1980*)

SUMMARY

1. Inactivation ('immobilization') of the non-linear component of capacitive current in semitendinosus muscles of *Rana pipiens* was studied using the three-micro-electrode voltage-clamp technique (Adrian, Chandler & Hodgkin, 1970).

2. The steady-state voltage dependence of non-linear charge immobilization was determined by changing the holding potential. The data were fitted to an equation analogous to that used to describe the charge activation process (Schneider & Chandler, 1973). The steepness parameter, k, is the same for charge activation and immobilization, but the mid-point voltage of charge immobilization is $8{\cdot}9 \pm 2{\cdot}6$ mV ($n = 9$) more negative than the mid-point of the non-linear charge activation curve. The charge relaxation rate constants are unaffected by changes in holding potential.

3. The time course of non-linear charge immobilization was studied using a protocol that measures the change in capacitive current required for a voltage step of a fixed magnitude determined before and after an intervening period of depolarization. The sum of the non-linear charge that is immobilized and the non-linear charge that remains mobile after a prolonged (> 1 s) depolarization is equal to the total non-linear charge measured at a normally polarized holding potential (-80 mV). The determination of the quantity of charge immobilized does not require the assumption of linearity of the control capacity transient.

4. The exponential time constant of charge immobilization was found to be steeply voltage dependent. The charge immobilization time constant was 4·4 s at -40 mV, 1·5 s at -20 mV and 0·28 s at $+20$ mV. Temperature was 5 °C.

5. In addition to a decrease in the magnitude of non-linear capacitive charge during prolonged depolarization muscle fibres generally showed an apparent decrease in linear effective capacity. It is suggested that this apparent change and the increase previously reported to occur when chronically depolarized fibres are hyperpolarized (Rakowski, 1978*a*) are artifactual results of incorrect current scaling rather than changes that result from alteration of a conductance pathway from the transverse tubular system into the sarcoplasmic reticulum.

INTRODUCTION

Schneider & Chandler (1973) observed a non-linear component of capacitive current in skeletal muscle. This phenomenon has been called 'membrane charge

movement' and has been suggested to play a role in the gating of calcium release from the sarcoplasmic reticulum of skeletal muscle (Schneider & Chandler, 1973; Chandler, Rakowski & Schneider, 1976*b*). It has been shown that there is a close correspondence between charge movement and the intracellular free calcium transient measured using the dye antipyralazo III (Kovacs, Rios & Schneider, 1979). Previous investigations (Adrian, Chandler & Rakowski, 1976; Adrian & Rakowski, 1978; Rakowski, 1978*a*) have focused on the non-linear membrane charge that is immobilized by maintained depolarization and that recovers on hyperpolarization as the most likely to be involved in contractile activation. Two reviews are available for a more complete discussion of this subject (Almers, 1978; Adrian, 1978).

The data reported in this study examine the process of non-linear charge immobilization in frog skeletal muscle. The results are presented in three parts. Part I reports the results of experiments conducted to examine the steady-state characteristics of charge immobilization by changing the holding potential. Part II investigates the kinetics of charge immobilization and Part III examines the apparent change in linear effective capacity that is produced by prolonged depolarization.

Two abstracts reporting the results of some of these experiments have been published (Rakowski, 1978*b*, *c*).

METHODS

The experimental methods have been described in detail (Rakowski, 1978*a*). The present experiments differ from those previously reported with respect to the experimental solution used, the initial holding potential and the voltage pulse protocol. The experimental apparatus, method of data collection and method of charge analysis are identical to those described previously.

The experimental solution used in this study has the following composition: rubidium chloride, 5 mM; tetraethylammonium chloride, 117·5 mM; calcium chloride, 1·8 mM; sucrose, 467 mM; tetrodotoxin, 2×10^{-7} M, pH = 7·1. This solution is identical to that used by Chandler, Rakowski & Schneider (1976*a*) except that 1·5 mM-sodium phosphate buffer is used here instead of Tris maleate. Passive electrical properties in this solution are similar to those previously reported (Chandler *et al.* 1976*a*). The initial holding potential usually was −80 mV.

The voltage pulse protocols used to obtain test and control capacity current transients are of two basic types. The first strategy is identical to that used by Chandler *et al.* (1976*a*). Control voltage steps are made at very negative voltages and are linearly scaled and subtracted from test voltage steps that are made in the depolarizing direction. The second subtraction technique is to obtain control and test capacity current transients over the same voltage range before and after an intervening event. Adrian *et al.* (1976), Adrian & Rakowski (1978) and Rakowski (1978*a*) have used this method to investigate the effects of long-duration prepulses on charge movements. One of the objects of the present study is to show that both methods give similar results.

All of the points at the 'on' and 'off' of experimental records are shown in the Figures presented here. No points have been omitted. The d.c. offset of subtracted records is also retained in the Figures. No base line subtraction has been performed on the experimental records shown.

RESULTS

Part I. Steady-state measurements using linear scaling

Non-linear charge immobilization

The steady-state relationship between membrane potential and the amount of non-linear membrane charge that remains mobile can be investigated by subtraction

of test and control capacitive current records at various holding potentials. In the records shown in Fig. 1 the holding potential was varied from −100 to −20 mV in 10 mV increments allowing a 2 min wait at each holding potential before data collection. There is a progressive reduction in the magnitude of the non-linear component of capacitive current observed for test steps over the range −100 to −20 mV as the holding potential is made more positive.

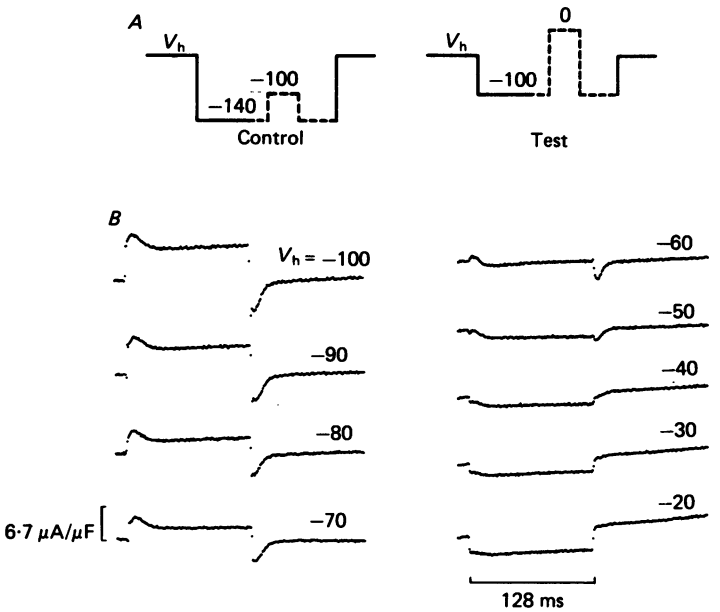

Fig. 1. Effect of holding potential on membrane charge movement. *A*, control and test pulse protocol for various holding potentials (V_h). The dashed lines indicate the period of data sampling used to obtain the records shown below. *B*, records of ΔV (test − control) are shown for a fibre held at the potential indicated beside each trace (mV). Fibre 33.2. Temperature 5 °C. The vertical scale corresponds to a ΔV magnitude of 10 mV. Each point represents a 1 ms time interval. Four control steps were signal-averaged, scaled and subtracted from each test step.

The steady-state charge immobilization relationship determined from three separate determinations at each holding potential for the fibre of Fig. 1 is shown in Fig. 2. The magnitude of the charge was determined by subtracting a sloping base line from the data and numerically integrating the result (Chandler *et al.* 1976*a*). The mean values of the data were fitted to the following equation:

$$Q = Q_{max}/[1+\exp(V_h - V^*)/k], \quad (1)$$

where Q (nC/μF) is the non-linear charge that remains mobile at various holding potentials, V_h(mV). The constants Q_{max}, V^* and k are free parameters determined by a least-squares fit to the data. For the data shown in Fig. 2 the best-fit values of these parameters were $V^* = -41{\cdot}6$ mV, $k = 10{\cdot}5$ mV and $Q_{max} = 30{\cdot}3$ nC/μF.

Comparison of charge activation and immobilization curves in the same fibre

The data shown in Fig. 3 present a comparison of non-linear charge transient areas determined for depolarizing steps from an initial holding potential of −80 mV and the non-linear charge that remains mobile determined from various holding potentials. The mean values of the 'on' and 'off' areas for the open symbols have been fitted to the following equation (Schneider & Chandler, 1973):

$$Q = Q_{max}/[1+\exp(V'-V_m)/k], \quad (2)$$

where Q (nC/μF) is the integral of the non-linear charge transients for voltage steps to various membrane potentials, V_m(mV), plotted on the abscissa. Q_{max}, V' and k are free parameters determined by a least-squares fit to the data.

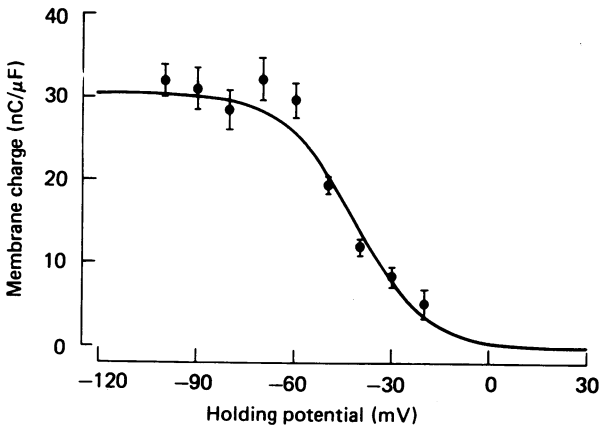

Fig. 2. Steady-state charge immobilization relationship. The mean values of three determinations of 'on' and 'off' charge transient areas from data taken as shown in Fig. 1 are plotted here as a function of the holding potential. The error bars represent ± 1 S.E.M. The theoretical curve was determined by a least-squares fit of the data to eqn. (1). Fibre 33.2. Temperature 5 °C.

The filled symbols in Fig. 3 were determined from the non-linear charge transients that remain mobile at various holding potentials, using a pulse protocol and subtraction procedure identical to that used to obtain the data in Figs. 1 and 2. The magnitude and voltage range of the control steps are identical for both the open and filled symbols in Fig. 3.

The data in Fig. 3 are similar to data published by Adrian & Almers (1976*b*, their Fig. 9).

Summary of the parameters Q_{max}, V^*, V' and k determined in various fibres

It was seldom possible to determine the activation Q *vs.* V curve and also obtain sufficient data to determine the steady-state charge immobilization curve in the same fibre. There was essentially no difference between the values of V^* and V' for the data shown in Fig. 3; however, in three other fibres the parameter V^* was more negative than V' by 3·4, 4·7 and 9·7 mV. A comparison of the mean values of the

charge activation and immobilization parameters from all of the fibres for which at least one set of data could be determined gives the following results. Normal charge activation Q *vs.* V data were obtained in twenty-four fibres. The mean parameter values are: $V' = -32{\cdot}1 \pm 1{\cdot}3$ mV; $k = 11{\cdot}1 \pm 0{\cdot}7$ mV, $Q_{max} = 23{\cdot}3 \pm 1{\cdot}7$ nC/μF and $\alpha' = 0{\cdot}032 \pm 0{\cdot}003$ ms^{-1} (cf. eqn. (3)). The steady-state charge immobilization curve

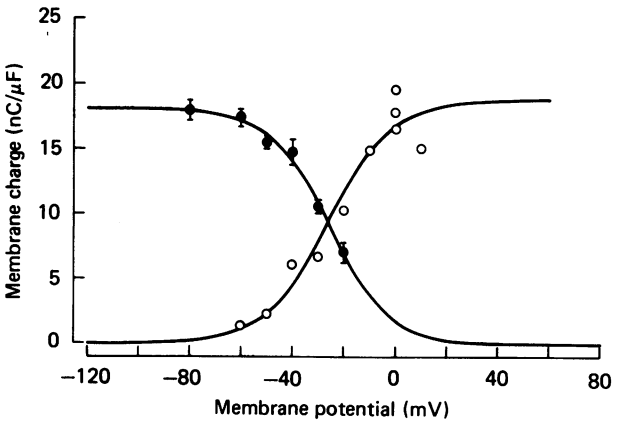

Fig. 3. Steady-state membrane charge activation and immobilization curves determined in the same fibre. ○, mean values of 'on' and 'off' membrane charge transient areas from records of ΔV (test − control). Four control pulses from −140 to −100 mV were scaled and subtracted from a test pulse from −100 mV to the test pulse voltage plotted on the abscissa. Holding potential, −80 mV. ●, mean values of three determinations of charge transient areas for test pulses from −100 to 0 mV at various holding potentials plotted on the abscissa. The theoretical curve drawn through the (○) was determined by a least-squares fit to eqn. (2). The best-fit parameters are $V' = -25{\cdot}7$ mV, $k = 12{\cdot}3$ mV and $Q_{max} = 18{\cdot}8$ nC/μF. The best-fit parameters for the (●) and eqn. (1) are $V^* = -25{\cdot}2$ mV, $k = 11{\cdot}4$ mV and $Q_{max} = 18{\cdot}0$ nC/μF. Fibre 37.6. Temperature 5 °C.

was determined in nine fibres. The mean parameter values are: $V^* = -41{\cdot}0 \pm 2{\cdot}6$ mV, $k = 12{\cdot}4 \pm 1{\cdot}3$ mV and $Q_{max} = 23{\cdot}6 \pm 3{\cdot}1$ nC/μF. The values of Q_{max} and k are not significantly different for these two sets of data ($P > 0{\cdot}5$); however, the parameters V^* and V' are statistically significantly different ($0{\cdot}01 < P < 0{\cdot}001$). These data suggest that the immobilization parameter V^* is slightly more negative than the value of V' determined from the normal Q *vs.* V distribution.

Comparison of non-linear charge activation curves at two different holding potentials

The simple expectation that charge that has become immobilized will not affect the voltage dependence of non-linear charge that remains mobile is tested in the experiment illustrated in Fig. 4. In this experiment the normal non-linear charge distribution function was determined initially at a holding potential of −80 mV. The same subtraction technique was used for data obtained at a holding potential of −45 mV. At this holding potential approximately half of the non-linear membrane charge should be immobilized. Following the measurements at $V_h = -45$ mV the holding potential was returned to −80 mV and a second set of determinations was done that incidentally illustrates saturation of the Q. *vs.* V curve for very positive

test potentials. The presence of small residual delayed ionic currents in early runs of an experiment make this demonstration difficult. However, the block produced by tetraethylammonium ions is more complete at the end of a long experimental protocol.

The best-fit parameters for the data in Fig. 4 indicate little change in the steepness parameter, k, under the two experimental conditions, but the maximum amount of

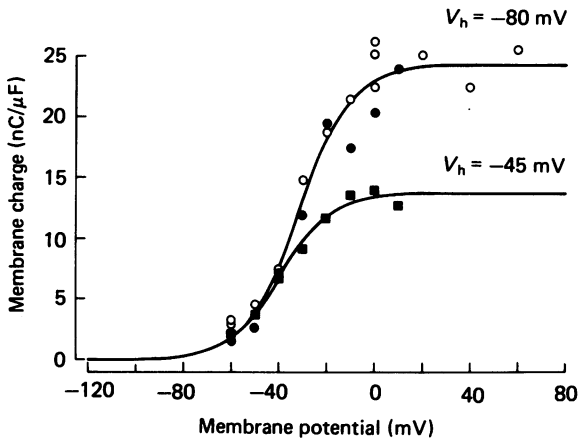

Fig. 4. Determination of the membrane charge distribution function following partial immobilization. ●, ΔV (test−control) transient areas of non-linear membrane charge movement determined from an initial holding potential of −80 mV. ■, charge transient areas determined 3 min after changing the holding potential to −45 mV. ○, charge transient areas determined 3 min after restoring the holding potential to −80 mV. The best-fit parameters to eqn. (2) for the data at $V_h = -80$ mV are $V' = -31{\cdot}7$mV, $k = 11{\cdot}3$ mV and $Q_{max} = 24{\cdot}4$ nC/μF. The best-fit parameters for the data at $V_h = -45$ mV are $V' = -39{\cdot}0$ mV, $k = 11{\cdot}1$ mV and $Q_{max} = 13{\cdot}8$ nC/μF. Fibre 34.7. Temperature 5 °C.

non-linear charge observed at $V_h = -45$ mV is reduced to 57% of that seen at $V_h = -80$ mV. In addition, there is a shift of the parameter V' in the hyperpolarizing direction (−7·3 mV). In two similar experiments shifts of only −4·1 and −2·6 mV were observed. The conclusion is, therefore, that charge immobilization has no substantial effect on the remaining mobile charge except possibly for a small shift of the parameter V'.

Comparison of the relaxation kinetics of non-linear charge measured at different holding potentials

The prediction based on independent movement of individual charged groups is that not only the steady-state distribution but also the kinetics of the transition of membrane charge should be unaffected by the presence of substantial immobilized charge. This prediction is supported by the data shown in Fig. 5. The normal non-linear charge transients measured at a holding potential of −80 mV have been fitted to a single exponential and a sloping base line as previously described by Chandler *et al.* (1976*a*). The reciprocal of the exponential time constant is plotted in Fig. 5 as a

function of membrane potential using data from fibre 34.7. The filled symbols have been fitted to eqn. (3) (Chandler *et al.* 1976*a*; Almers & Best, 1976).

$$\alpha = \frac{\alpha'(V_m - V')}{k} \coth \frac{(V_m - V')}{2k}, \tag{3}$$

where α (ms^{-1}) is the relaxation rate constant measured for non-linear charge movement at various membrane potentials, V_m(mV). V' and k can be determined

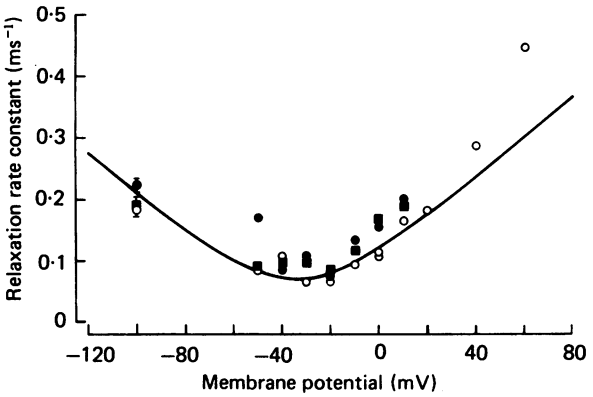

Fig. 5. Comparison of membrane charge relaxation kinetics at $V_h = -80$ mV and -45 mV. The reciprocals of the time constants of charge transients measured in Fig. 4 are plotted here as a function of the membrane potential. ●, data measured at $V_h = -80$ mV; ■, data measured 3 min after changing V_h to -45 mV; ○, data measured 3 min after restoring V_h to -80 mV. The mean value of the 'off' rate constant is plotted for $V_m = -100$ mV. The error bars indicate ± 1 S.E. The curve is drawn according to eqn. (3) with parameters $V' = -34{\cdot}5$ mV, $k = 11.1$ mV and $\alpha' = 0{\cdot}0359$ ms^{-1}. Fibre 34.7. Temperature 5 °C.

from the charge distribution function and α' is the only remaining free parameter. The value of α' determined by a least-square fit of the data at a holding potential of -80 mV is 0·0359 ms^{-1}. The data for a holding potential of -45 mV give a value of α' of 0·0364 ms^{-1}. These values are sufficiently similar to support the suggestion that there is no significant alteration in the relaxation kinetics of non-linear charge movement as a result of partial charge immobilization.

It also should be noted that the above analysis is oversimplified in some important respects. Adrian & Almers (1976*b*) and Adrian & Peres (1979) have reported more complex kinetic behaviour of charge movements in muscle and have commented on the asymmetrical shape of the charge distribution function. No attempt has been made in this study to examine closely the kinetic behaviour in a way that would bring out the features commented on by these other investigators. The fact that the charge distribution curves appear to be quite symmetrical, however, while the curves of Adrian & Almers (1976*b*) and Adrian & Peres (1979) are, at times, distinctly asymmetrical suggests that there may be methodological or other differences that account for the difference. One possibility, for example, is the fact that substantially higher osmolarity experimental solutions have been used in this and an earlier study (Chandler *et al.* 1976*a*). Recent unpublished results in this laboratory using an experimental solution and pulse protocol identical to that used by Adrian & Peres (1979) confirm the existence of additional kinetic complexities in the time course of non-linear charge movement. In the absence of the necessary additional information, however, it seems most

appropriate to treat the present data in the simplest fashion as has been done here and to be aware that additional kinetic complexities may exist.

Part II. Transient changes in total capacitive charge requirement

The determination of immobilized charge does not require the assumption of linearity of the control pulse

The results presented in Part I were determined using steady-state measurements of the amount of non-linear charge remaining at various holding potentials. The subtraction method depended on the determination of a linear scaling factor. The

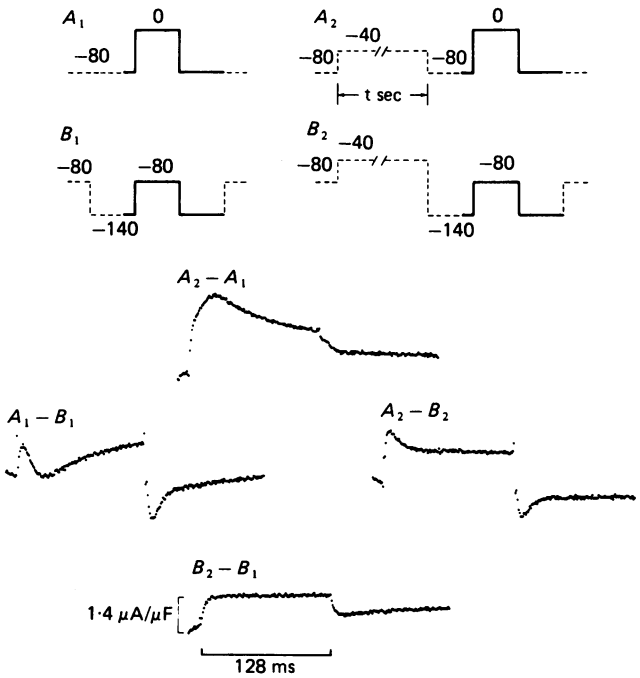

Fig. 6. The determination of changes in capacity following prolonged depolarization. Subtraction of the capacity transients that are obtained in response to the four pulse sequences illustrated gives rise to difference records that are defined as follows: non-linear charge, $A_1 - B_1(V_A/V_B)$; change in total charge, $A_2 - A_1$; remaining non-linear charge, $A_2 - B_2(V_A/V_B)$; change in linear charge, $B_2 - B_1$. Subsequent references to records of this type will omit the voltage scaling factor, $f = V_A/V_B$, for simplicity. In this example $f = 80/60$. The actual magnitude of the individual voltage steps was measured and a scaling factor was calculated for each record. Records of the initial non-linear charge and changes in capacity current following a 2 s depolarization at 0 mV using a pulse protocol of this kind are shown in the lower half of the Figure. Fibre 27.4. Temperature 4·7 °C. The vertical scale corresponds to a ΔV magnitude of 5 mV.

linearity of the capacitive current in the control pulse is an assumption that requires experimental verification by other methods. On the other hand, the protocol used to determine the recovery of membrane charge (Adrian *et al.* 1976; Rakowski, 1978*a*) simply subtracts ΔV records obtained over the same voltage range before and after a long-duration prepulse. Charge immobilization can be studied in a similar way. If

the ΔV transients resulting from the voltage steps labelled A_2 and A_1 in Fig. 6 are subtracted, the resulting difference is simply the change in the total capacitive current that is a result of the prepulse. Since the voltage excursions in A_1 and A_2 are identical in magnitude and cover the same voltage range, no scaling factor is required and the assumption of linearity is not necessary.

The experimental records shown in Fig. 6 show the non-linear membrane charge present at a normal holding potential (A_1-B_1), the non-linear charge remaining after a 2 s depolarizing prepulse to 0 mV (A_2-B_2), the change in total capacitive charge required for a test step from -80 to 0 mV (A_2-A_1), and the change in capacitive charge required for control steps from -140 to -80 mV (B_2-B_1). There is a decrease in the early transient charge movement and a decline in the residual delayed outward ionic current after the prolonged depolarization (compare A_1-B_1 with A_2-B_2). Note that the result of the subtraction A_2-A_1 gives a negative initial current transient. This indicates that there is a net decrease in the total charge required for the voltage step from -80 to 0 mV after the prolonged depolarization. The change in total charge (A_2-A_1) consists of at least two components. It can be seen directly that the non-linear component of membrane charge has decreased by comparison of A_1-B_1 with A_2-B_2. The capacitive charge required for the control step is reduced by the prolonged depolarization since the record B_2-B_1 has an initially negative ΔV transient. It is clear, therefore, that both non-linear membrane charge movement and the apparent linear effective capacity of the muscle fibre are reduced by prolonged depolarization.

Comparison of the kinetics of normal non-linear charge movement with the kinetics observed for protocol A_2-A_1

The relaxation rate constants for normal non-linear charge obtained using the protocol A_1-B_1 were fitted to eqn. (3) using values of V' and k obtained from the steady-state distribution of normal charge movement for the fibre studied. The parameter α' was determined by a least-squares fit to be 0·0186 ms^{-1}. Records of the type A_2-A_1 were obtained in which the test pulse voltage was varied in a series of determinations each of which was preceded by a 16 s depolarization to 0 mV. The first ten points after the step were excluded from the curve-fitting procedure. The analysis, therefore, included only transient current components with time constants comparable to those observed for non-linear membrane charge. A least-squares fit of these data to eqn. (3) using the steady-state values of V' and k determined previously gave a value of α' of 0·0181 ms^{-1}. The close agreement of the value of α' determined by these two different techniques supports the suggestion that the slow component of the A_2-A_1 protocol is a result of the immobilization of non-linear charge.

The voltage distribution of non-linear charge remaining after partial immobilization

We can examine the behaviour of the remaining non-linear charge following a prolonged depolarization from records of the type A_2-B_2 and compare these results with normal non-linear charge (A_1-B_1). An experiment was done to compare the voltage distribution function of normal non-linear charge with the Q *vs.* V relationship following 2 s depolarizations at -20 mV. Comparison of the least-squares fits of the normal data and the data obtained following 2 s depolarizations at -20 mV show a reduction of Q_{max} to 39% of its normal value and a shift of

the parameter V' of $-3{\cdot}7$ mV. This small negative shift in the mid-point of the voltage distribution function is consistent with the shift observed previously using changes in holding potential (Fig. 4). The data obtained from the time course of the charge transients after a 2 s prepulse to -20 mV agree with the relaxation rate constants determined from a holding potential of -80 mV. The least-squares fit to eqn. (3) of data obtained at $V_h = -80$ mV gives a value of the parameter α' of $0{\cdot}0321$ ms^{-1}. If the data following 2 s depolarization at -20 mV are fitted in the same way the value of α' is $0{\cdot}0346$ ms^{-1}. Since each charge transient returned to the same potential at the 'off' of the test step, we can make a comparison of the values of the relaxation rate constants observed at a normal holding potential of -80 mV and after a 2 s prepulse at -20 mV. The 'off' rate constants are not statistically significantly different ($0{\cdot}5 > P > 0{\cdot}2$).

Summary of kinetic data obtained after changes in holding potential and after prepulses

The data described above support the previous observation obtained by measurements at various holding potentials. Prolonged depolarization produces a reduction in the magnitude of mobile non-linear membrane charge. This process of charge immobilization is accompanied by small hyperpolarizing shifts of the Q. *vs.* V curve of non-linear charge that remains mobile. However, it is not necessary to alter the steady-state parameters V' and k to obtain satisfactory fits to the relaxation kinetics of non-linear charge. There is consistent agreement between the relaxation kinetics of normal charge, the slow component of the change in total charge (data not shown), the non-linear charge that remains mobile after a change in holding potential (Fig. 5) and the charge that remains mobile after partial immobilization by a prepulse (data not shown). The non-linear charge translocation or dipole rotation process appears to be unaffected by charge immobilization except possibly for a small shift of the voltage dependence in the hyperpolarizing direction.

Time course of non-linear charge immobilization determined from records of remaining non-linear charge ($A_2 - B_2$)

The records in Fig. 7 show the time course of non-linear charge immobilization for a depolarizing prepulse to -40 mV. The data in Fig. 7 can be analysed by computing the transient area of the remaining charge and plotting the result as a function of the prepulse duration. This has been done for three different prepulse voltages in Fig. 8. In order to obtain an estimate of the immobilization rate constant, the value observed at 16 s has been arbitrarily taken to be the steady state and the data have been fitted to an equation for a single exponential decay process. The data from this fibre indicate that charge immobilization is very steeply voltage dependent. In particular, note that prepulses to $+20$ mV produce complete immobilization in about 1 s.

Additional experiments have been done on two other fibres with comparable results, but the data shown in Fig. 8 are the most complete set of records from any fibre. The data are extremely difficult to obtain using the $A_2 - B_2$ protocol because of the necessity of a prolonged recovery period of up to 5 min after each pulse. The technique originally used by Chandler *et al.* (1976*b*) to determine the immobilization and recovery time course is more efficient at the small sacrifice of a slight difference in the timing of control and test pulses to be subtracted.

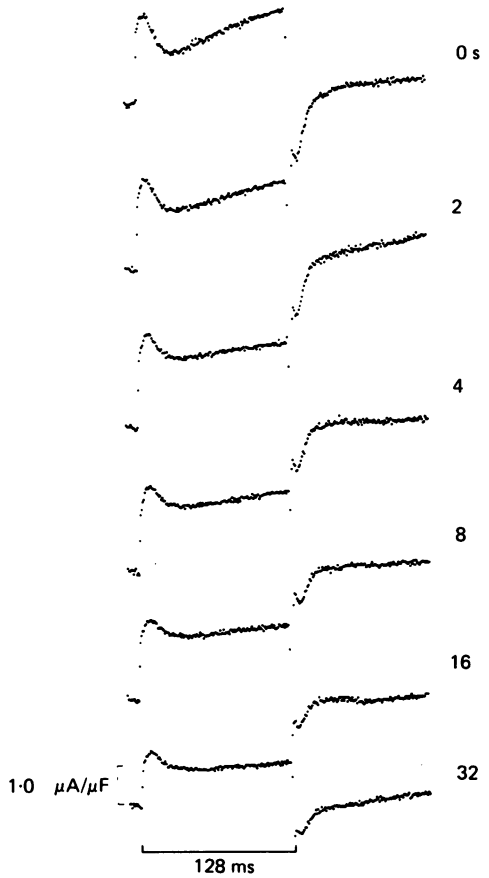

Fig. 7. The time course of non-linear charge immobilization. A series of records of non-linear charge remaining after prolonged depolarization to −40 mV using the protocol A_2-B_2 are shown above. The numbers at the right of each record indicate the duration of the depolarizing prepulse at −40 mV. The test voltage excursion for each record was from −80 to 0 mV as illustrated in Fig. 6. The initial record (0 s) shows a large quantity of non-linear charge and substantial delayed ionic current. These diminish as the duration of the prepulse to −40 mV is prolonged, but note particularly that a substantial amount of non-linear charge remains even after a 32 s prepulse. Fibre 27.5. Temperature 4·6 °C. The vertical current scale corresponds to a ΔV magnitude of 5 mV.

Part III. Apparent changes in linear capacity after prolonged depolarization

Changes in linear capacity are not always observed

A possible explanation for the observation of a decrease in linear capacity is that the result is simply a technical fault or artifact of the method. This possibility is raised most strongly by the observations shown in Fig. 9. There is substantial non-linear charge present initially for a test step from −80 to 0 mV (A_1-B_1). Following the depolarization, there is a small but measurable remaining non-linear charge (A_2-B_2). If we subtract the value of the non-linear charge that remains (5·7 nC/μF) from the total non-linear charge initially present (25·0 nC/μF), the difference (19·3 nC/μF) is

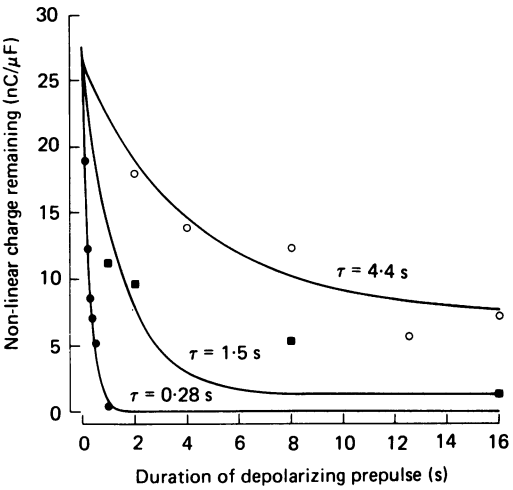

Fig. 8. Non-linear charge immobilization time course at various membrane potentials. The integral of the non-linear charge transients shown in Fig. 7 and additional data from the same fibre are shown here as a function of the duration of the depolarizing prepulse. Prepulse voltages: ○, −40 mV; ■, −20 mV; and ●, +20 mV. The initial value of non-linear charge was determined from the mean value of the determinations at $t = 0$ to be 26·6 nC/μF. A least-squares fit to the data gives exponential time constants (τ) for immobilization of 4·4 s at −40 mV, 1·5 s at −20 mV and 0·28 s at +20 mV. The steady-state value of non-linear charge is estimated from the value at 16 s to be 7·3 nC/μF at −40 mV and 1·3 nC/μF at −20 mV. Fibre 27.5. Temperature 4·6 °C.

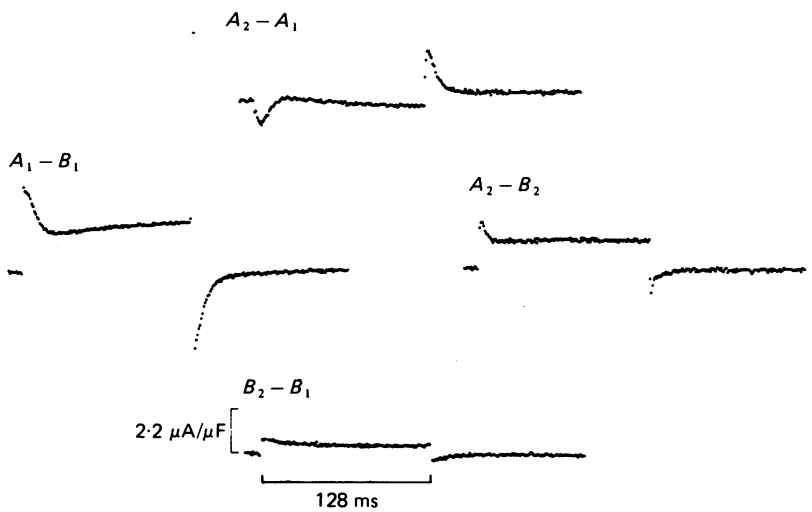

Fig. 9. Example of a fibre in which no apparent change in linear capacity occurred following prolonged depolarization. The records shown above follow the protocol illustrated in Fig. 6 except that the prolonged depolarization in A_2 and B_2 was done at a membrane potential of 0 mV for 16 s. The estimates of non-linear charge and the charge following prolonged depolarization are as follows: non-linear charge $(A_1 - B_1) = 25{\cdot}0$ nC/μF; change in total charge $(A_2 - A_1) = -19{\cdot}6$ nC/μF; remaining non-linear charge $(A_2 - B_2) = 5{\cdot}7$ nC/μF. Fibre 23.1. Temperature 4·4 °C. The vertical current scale corresponds to a ΔV magnitude of 5 mV.

the predicted amount of non-linear charge that has been immobilized by the prepulse. This is very nearly equal in absolute magnitude to the mean value of the 'on' and 'off' integrals of the A_2-A_1 trace ($-19{\cdot}6$ nC/μF). Note in particular that there is no rapid transient observed in the trace B_2-B_1 and, therefore, no change in the apparent linear effective capacity despite the fact that in this fibre the non-linear

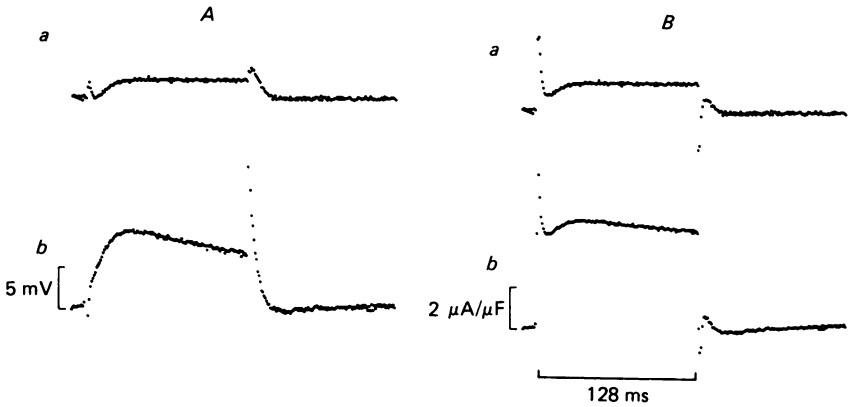

Fig. 10. Recalculation of subtracted records suggests that the apparent changes in linear capacity are an artifact. *Aa*, change in the total capacitive charge requirement for a voltage step from -80 to 0 mV following a prepulse to 0 mV for 16 s (protocol A_2-A_1). *Ab*, after an experimental protocol lasting 37 min the pulse sequence in *Aa* was repeated with the apparent result that there is now both a decrease in linear capacity as well as the change in non-linear charge originally observed. *Ba*, the control and test ΔV records that were subtracted in *Aa* have each been scaled by individually determined values of $2p/3\,l^2r_i\,c_m$. The subtracted result is shown. *Bb*, the control and test ΔV records of *Ab* have been scaled by individually determined values of $2p/3\,l^2r_i\,c_m$. The subtracted result is shown. Fibre 26.7. Temperature 4·3 °C. Both vertical current scales correspond to a control pulse ΔV magnitude of 5 mV.

charge has been reduced to about 23 % of its initial value by the depolarizing prepulse. This fibre provides an example in which a decrease in non-linear charge movement is observed without an accompanying decrease in linear effective capacity.

Recalculation of traces of the type A_2-A_1 based on the assumption that no change in linear effective capacity has occurred

The data that result from subtraction of ΔV transients using the charge immobilization protocol may be re-examined as shown in Fig. 10. The data in column *A* were obtained using the protocol A_2-A_1 following a 16 s prepulse to 0 mV. The record *Aa* was obtained at the outset of the experiment and record *Ab* was obtained using the identical voltage excursions after the micro-electrodes had been in place for 37 min. Record *Aa* is similar to record A_2-A_1 in Fig. 9 in that the area of the transient approximately satisfies the equality required among the values for total non-linear charge (21·3 nC/μF), and the sum of the non-linear charge remaining (11·5 nC/μF) and the reduction in the total capacitive charge (14·9 nC/μF) (data not shown). On the other hand, record *Ab* shows a remarkable apparent increase in the transient area as well as a substantial shift in the steady base line level of current.

This pattern suggests that there has been a change in the current scaling factor during the experiment giving rise to artifactual changes when the ΔV traces are subtracted. This is supported by the similar appearance of records *Ba* and *Bb*. The control and test capacitive transients that were subtracted to obtain these records have been scaled by individual values of the factor $2p/3\,l^2 r_i\,c_m$ (Adrian *et al.* 1970). That is, the individual values of the scaling factor were obtained by integration of the capacitive transient area of the control and the test step before subtraction. This forces the net transient area of the subtracted traces to be zero and permits one to examine the extent to which the control and test transients are not co-temporal. It is clear that record *Bb* has a much greater difference in the steady-state current during the pulse, suggesting that there is a greater leak conductance under the test condition. The fact that the residual biphasic current transients are very similar in time course suggests that there is a non-linear capacitive current component that is immobilized under both experimental conditions, but was partially obscured by the initial fast transient in record *Ab*.

The conclusion, then, is that record *Aa* represents the immobilization of non-linear charge, but that record *Ab* is the sum of the non-linear charge and an apparent decrease in linear effective capacity owing to a change in the current scaling factor. These changes may occur as a result of changes in electrode leak magnitude (Adrian & Almers, 1976*a*; Schneider & Chandler, 1976) or by a change in the fraction of the membrane potential measured by each electrode (see Appendix).

Capacitive transients measured in the voltage range -140 *to* -80 *mV are co-temporal if scaled so that the transient areas are equal*

If we examine data obtained using the protocol $B_2 - B_1$ there should be only a very small amount of non-linear charge present since the voltage excursion is over the range -140 to -80 mV and changes in 'charge 2' are not expected. The data shown in Fig. 11 examine this point. The data were obtained using the protocol $B_2 - B_1$ after a depolarizing prepulse to -40 mV for 8 s. The subtraction is shown in record (*A*) and is typical in that it shows an apparent decrease in the capacitive charge required for the step following the depolarization. Record (*B*) was obtained by scaling the individual control and test ΔV transients by the factor $2p/3\,l^2 r_i$ to examine whether the apparent change in capacity could be accounted for by a change in r_i. As can be seen in (*B*) the apparent reduction of linear capacity is smaller if this change in the current scaling factor is included in the calculation. However, the measured change in r_i does not completely eliminate the effect. In record (*C*) the test and control capacitive transients were scaled individually by the factor $2p/3\,l^2 r_i\,c_m$. It is clear that when the total areas of the test and control capacitive transients are made equal, the result upon subtraction shows that the data are very nearly co-temporal. The subtracted record (*C*) is flat. This strongly supports the validity of the statement that there is no actual change in the effective linear capacity of the muscle fibre produced by prolonged depolarization. The result rules out the suggestion that the change in linear capacity is a result of a change in the coupling resistance between the sarcoplasmic reticulum and transverse tubular system (Rakowski, 1978*a*; Mathias, Levis & Eisenberg, 1979, 1980).

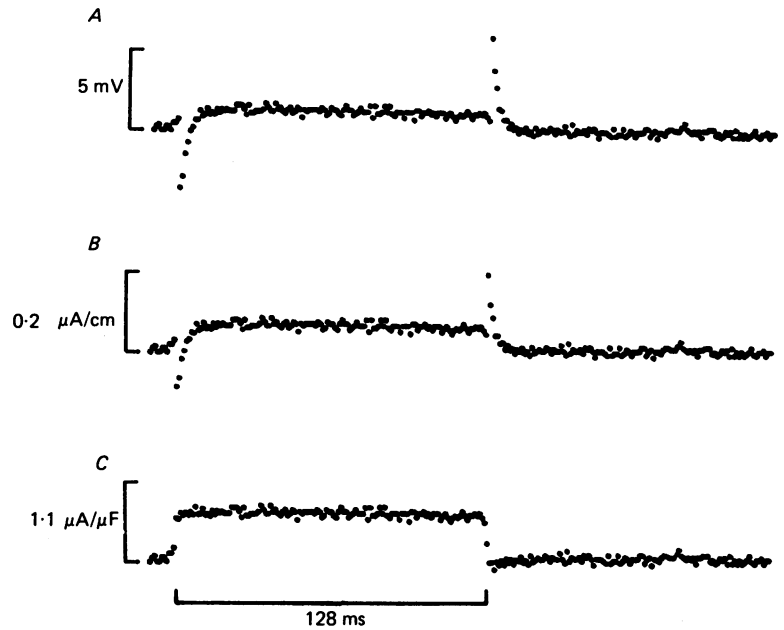

Fig. 11. An example of a record of an apparent decrease in linear capacitive charge in which a recalculation shows the test and control capacity transients to be co-temporal if the integrals of the traces are made equal. *A*, subtraction of ΔV transients for voltage steps from -140 to -80 mV before and after depolarization to -40 mV for 8 s gives an apparent decrease in the capacitive charge requirement (protocol B_2-B_1). *B*, the magnitude of the apparent change is only slightly reduced if the individual control and test ΔV transients are scaled by different values of $2p/3l^2r_i$ determined from the total current record for each trace before subtraction. *C*, the records of ΔV have been separately scaled by $2p/3l^2r_i c_m$ before subtraction. Since c_m is calculated from the ΔV transient integral of each trace, this procedure forces the integral of the subtracted result to equal zero, but also note that there is no residual positive and negative transient and that the scaled ΔV transients are co-temporal. This record, therefore, supports the conclusion that there is not a significant change in non-linear membrane charge in the voltage range from -140 to -80 mV and that the apparent change in the magnitude of the capacity transient is an artifact resulting from incorrect current scaling. Fibre 27.5. Temperature 4·6 °C. The vertical current scale corresponds to a control pulse ΔV magnitude of 5 mV for all three records.

DISCUSSION

The steady-state data are compatible with a three-state model of charge immobilization

Consider the following three-compartment model:

$$a \underset{k_{ba}}{\overset{k_{ab}}{\rightleftharpoons}} b \underset{k_{cb}}{\overset{k_{bc}}{\rightleftharpoons}} c, \tag{4}$$

where a represents charge in a 'resting' state at a normally polarized voltage, b is charge in an activated state and c is charge in an 'immobilized' state. The various rate constants, k_{ab}, k_{ba}, etc. are voltage-dependent rate constants for the transitions between these states.

The data shown in Fig. 3 can be represented by the following steady-state distribution of charge among three states at a holding potential equal to the value of the mid-point parameter for the charge immobilization curve ($V_h = V^*$): $a+b = \frac{1}{2}Q_{max}$, $c = \frac{1}{2}Q_{max}$.

Let us consider a simple one-barrier exponential model for the transitions from b to c. The rate constants are as follows:

$$k_{bc} = A \exp[(V - V^*)/k] \quad (5)$$

$$k_{cb} = A \exp[-(V - V^*]/k], \quad (6)$$

where A is the rate constant at the transition potential for immobilization, V^*, for which $k_{bc} = k_{cb}$ and k is the e-fold steepness parameter defined for charge activation by eqn. (2).

At a holding potential $V_h = V = V'$ we may substitute in eqn. (5) and (6) and obtain eqn. (7):

$$V' - V^* = \frac{k \ln (k_{bc}/k_{cb})}{2}. \quad (7)$$

The difference in the transition potentials ($V^* - V'$) required to produce the steady-state distribution condition $2b$ approximately equal to c is, therefore, $[(-k \ln 2)/2]$. For a mean value of $k = 11$ mV the difference is only $-3{\cdot}8$ mV. This value is comparable to the observed differences in the parameters V^* and V' measured in these experiments. This simple three-state model of charge immobilization is compatible with the observed intersection of the steady-state charge immobilization curve and activation Q *vs.* V curve.

The movement and immobilization of membrane charge is consistent with independent movement of charged subunits

The translocation of charged groups or reorientation of permanent dipoles within the membrane upon depolarization will increase the potential energy required for the transition of subsequent charged groups provided that the groups are sufficiently closely spaced that they can interact electrostatically. A calculation of the change in surface potential can be used to determine the increase in the transmembrane potential gradient expected as a result of the translocation of membrane charge. If we take an average value for membrane charge density of 25 nC/cm^2 and a value of 1 μF/cm^2 for membrane capacity (Schneider, 1970; Hodgkin & Nakajima, 1972) the change in surface charge density produced by membrane charge translocation across the total (surface and tubular) membrane area is 1560 e/μm^2. For charged groups having a valence of +3 this corresponds to a density of 520 groups/μm^2 and a linear spacing of 44 nm between charged groups. A similar calculation has been made by Schneider & Chandler (1973) who obtained a somewhat lower density based on their measurements. For 300 mM-uni-univalent electrolyte the change in surface potential at each membrane-solution interface can be calculated to be +0·2 mV. The overall increase in the potential gradient is, therefore, only about +0·4 mV. The data, however, indicate that there is no significant shift of the voltage dependence of charge activation in the depolarizing direction. The measured shift in the mid-point parameter of charge activation is in the opposite direction (Fig. 4).

The same reasoning can be applied to the process of charge immobilization. If the

transition from the activated to immobilized state is a result of the translocation of an oppositely charged immobilizing group across the membrane, the process of charge immobilization should result in a further shift of the mid-point parameter in the positive direction. Models of this kind are inconsistent with the data that indicate voltage shifts in the hyperpolarizing direction. The conclusion is that electrostatic interaction between charged groups does not account for the observed shifts in mid-point parameters and that the data are consistent with independent movement of charged groups within the membrane and do not necessitate invoking electrostatic interaction between mobile charged groups.

The apparent decrease in linear effective capacity after prolonged depolarization is an artifact

The decrease in 'linear' effective capacity measured after prolonged depolarization is likely to be an artifact resulting from a change in the ΔV scaling factor. This conclusion is based on the following observations: (1) occasionally fibres do not show significant changes in linear effective capacity following depolarization (Fig. 9); (2) the magnitude of the observed change in linear effective capacity increases if a fibre is examined over a prolonged period of time (Fig. 10); and (3) if the capacitive transients measured before and after prolonged depolarization are scaled so that they are equal in area, subtraction of the records indicates that the scaled transients are co-temporal (Fig. 11). The last point is convincing. If a change in the effective capacity were to take place because of a change in the length constant of the transverse tubular system or as a result of an increase in the electrical resistance at the junction between the transverse tubular system and sarcoplasmic reticulum (Mathias *et al.* 1979, 1980), the time course of the capacitive transient would be altered as well as decreased in total area.

Failure of the V_1 and V_2 electrodes to monitor the full membrane potential

Adrian & Almers (1976*a*) and Schneider & Chandler (1976) have considered the effect of current leakage at the micro-electrode impalement sites on the determination of the effective membrane capacity. An upper limit can be placed on the magnitude of the leakage conductance at the V_1 electrode and used to obtain an estimate of the maximum error that will result from current leakage at the V_1 electrode. In these experiments as well as those reported by Schneider & Chandler (1976) the upper bound for the parameter K is 0·1 and, therefore, the upper limit of the error in determining the effective membrane capacity is about 2·5 %. Since the changes in linear effective capacity observed in these experiments and in previous work (Rakowski, 1978*a*) are as large as 30 %, a change in leakage conductance at the V_1 electrode penetration site is not a sufficient explanation of the observed change in linear effective capacity. Changes in leakage conductance at the V_2 and I electrodes have no effect on the determination of effective capacity.

The previous analysis of the effect of electrode leaks can be extended to consider the error produced by failure of the V_1 and V_2 electrodes to monitor the full membrane potential (see Appendix). The conclusion of this analysis is that failure at both the V_1 and V_2 electrodes can have an effect on the determination of the fibre effective capacity. For the special case in which the parameters f_1 and f_2 remain exactly equal

to each other, the errors will cancel. However, if only one of the two voltage electrodes fails, the error can be substantial.

Immobilizable and non-linear membrane charge are identical

It is particularly important to note that the data obtained using two different subtraction techniques are in agreement. It is clear in Fig. 9, for example, that the non-linear charge immobilized by maintained depolarization and measured by a method that does not assume linearity of the 'control' ΔV transient (A_2-A_1) gives the same result as can be determined from the total non-linear charge initially present (A_1-B_1) and that which remains following the depolarization (A_2-B_2). Under conditions that produce complete immobilization of membrane charge, this technique permits the direct comparison of the magnitude and time course of non-linear membrane charge with the charge that is immobilized. The results show that immobilizable and non-linear membrane charge are identical. The determination of immobilized charge does not require the assumption of linearity of the control capacity transient.

APPENDIX

The purpose of this section is to extend previous analyses (Adrian & Almers, 1976*a*; Schneider & Chandler, 1976) of the error introduced by current leakage at the micro-electrode impalement sites to consider the additional error that results from failure of the micro-electrodes to record the full membrane potential. This Appendix closely follows the nomenclature used by Schneider & Chandler (1976) and where possible the same system of notation is retained.

Modification of previously derived equations to account for electrode failure

The relationship between the measured membrane voltage (E) and the actual membrane voltage (V) at the two voltage electrodes is

$$E_1 = f_1 V_1 \tag{A 1}$$

and

$$E_2 = f_2 V_2, \tag{A 2}$$

where f_1 and f_2 represent the fractions of the actual membrane potential sensed by each electrode. Since changes in f_1 and f_2 do not change r_1, r_2 or the fibre admittance, the correction factors $p(l/\lambda)$ and $h(l/\lambda)$ are independent of f_1 and f_2. E_1/f_1 may be substituted for V_1 and E_2/f_2 may be substituted for V_2 in the equations derived by Schneider & Chandler (1976) for the parameters i_m, λ, r_i and c_{eff}. The substitution provides a means of estimating the error produced by f_1 and f_2 on the calculated value of these parameters; however, in the usual situation the actual magnitudes of f_1 and f_2 are not known.

The effect of a change in f_2 on the measured effective capacity

Eqn. (17*b*) of Schneider & Chandler (1976) is used to calculate a measured value of effective capacity (denoted by c'_{eff}). We may write eqn. (17*b*) for a test and control

voltage step as follows:

$$c'_{\text{eff}}(\text{test}) = \frac{2h(l/\lambda)}{3l^2 r_i E_1(\text{test}, \infty)} \int_0^\infty \Delta E_{\text{tr}}(\text{test})\, dt \tag{A 3}$$

$$c'_{\text{eff}}(\text{control}) = \frac{2h(l/\lambda)}{3l^2 r_i E_1(\text{control}, \infty)} \int_0^\infty \Delta E_{\text{tr}}(\text{control})\, dt. \tag{A 4}$$

Since $h(l/\lambda)$ is not a function of f_2, and $E_1(\text{test}, \infty) = E_1(\text{control}, \infty)$ for voltage control at $x = l$, the ratio of the measured effective capacities can be written

$$\frac{c'_{\text{eff}}(\text{test})}{c'_{\text{eff}}(\text{control})} = \frac{\int_0^\infty \Delta E_{\text{tr}}(\text{test})\, dt}{\int_0^\infty \Delta E_{\text{tr}}(\text{control})\, dt}. \tag{A 5}$$

The appropriate expressions for the transient part of the measured voltages are

$$\Delta E_{\text{tr}}(\text{test}) = E_2(\text{test}) - E_1(\text{test}) - E_1(\text{test})\left[\frac{E_2(\text{test}, \infty) - E_1(\infty)}{E_1(\infty)}\right] \tag{A 6}$$

and

$$\Delta E_{\text{tr}}(\text{control}) = E_2(\text{control}) - E_1(\text{control}) - E_1(\text{control}) \left[\frac{E_2(\text{control}, \infty) - E_1(\infty)}{E_1(\infty)}\right]. \tag{A 7}$$

For the case in which only f_2 changes in going from the test to control conditions we may write $E_1(\text{test}) = E_1(\text{control})$ and $E_2(\text{test})/f_2(\text{test}) = E_2(\text{control})/f_2(\text{control})$. Substituting these relationships in eqns. (A 5)–(A 7) we find a cancellation of terms to produce the simple result:

$$\frac{c'_{\text{eff}}(\text{test})}{c'_{\text{eff}}(\text{control})} = \frac{f_2(\text{test})}{f_2(\text{control})}. \tag{A 8}$$

The effect of a change in f_1 on the measured effective capacity

For the case in which only f_1 changes in going from the test to control conditions, we may write

$$E_2(\text{test}) = \frac{f_1(\text{control})}{f_1(\text{test})} E_2(\text{control}) \tag{A 9}$$

for the condition $f_2(\text{test}) = f_2(\text{control})$. Substituting eqn. (A 9) in eqns. (A 5)–(A 7) produces the following result upon simplification:

$$\frac{c'_{\text{eff}}(\text{test})}{c'_{\text{eff}}(\text{control})} = \frac{f_1(\text{control})}{f_1(\text{test})}. \tag{A 10}$$

Eqns. (A 8) and (A 10) are comparable. Eqn. (A 8) predicts the ratio of measured effective capacities when f_2 changes in the interval between the test and control voltage pulses, while eqn. (A 10) predicts the ratio expected when f_1 changes.

This work was supported by a grant to the Jerry Lewis Neuromuscular Research Center at Washington University from the Muscular Dystrophy Association of America and by grant no. NS 14856 from the U.S. National Institutes of Health.

REFERENCES

ADRIAN, R. H. (1978). Charge movement in the membrane of striated muscle. *A. Rev. Biophys. Bioeng.* **7**, 85–112.

ADRIAN, R. H. & ALMERS, W. (1976*a*). The voltage dependence of membrane capacity. *J. Physiol.* **254**, 317–338.

ADRIAN, R. H. & ALMERS, W. (1976*b*). Charge movement in the membrane of striated muscle. *J. Physiol.* **254**, 339–360.

ADRIAN, R. H., CHANDLER, W. K. & HODGKIN, A. L. (1970). Voltage clamp experiments in striated muscle fibres. *J. Physiol.* **208**, 607–644.

ADRIAN, R. H., CHANDLER, W. K. & RAKOWSKI, R. F. (1976). Charge movement and mechanical repriming in striated muscle. *J. Physiol.* **254**, 361–388.

ADRIAN, R. H. & PERES, A. (1979). Charge movement and membrane capacity in frog muscle. *J. Physiol.* **289**, 83–97.

ADRIAN, R. H. & RAKOWSKI, R. F. (1978). Reactivation of membrane charge movement and delayed potassium conductance in skeletal muscle fibres. *J. Physiol.* **278**, 533–557.

ALMERS, W. (1978). Gating currents and charge movements in excitable membranes. *Rev. Physiol. Biochem. Pharmac.* **82**, 96–190.

ALMERS, W. & BEST, P. M. (1976). Effects of tetracaine on displacement currents and contraction in frog skeletal muscle. *J. Physiol.* **262**, 583–611.

CHANDLER, W. K., RAKOWSKI, R. F. & SCHNEIDER, M. F. (1976*a*). A non-linear voltage dependent charge movement in frog skeletal muscle. *J. Physiol.* **254**, 245–283.

CHANDLER, W. K., RAKOWSKI, R. F. & SCHNEIDER, M. F. (1976*b*). Effects of glycerol treatment and maintained depolarization on charge movement in skeletal muscle. *J. Physiol.* **254**, 285–316.

HODGKIN, A. L. & NAKAJIMA, S. (1972). Analysis of the membrane capacity in frog muscle. *J. Physiol.* **221**, 121–136.

KOVACS, L., RIOS, E. & SCHNEIDER, M. F. (1979). Calcium transients and intramembrane charge movement in skeletal muscle fibres. *Nature, Lond.* **279**, 391–396.

MATHIAS, R., LEVIS, R. & EISENBERG, R. (1979). The charge movement expected from current flow into the sarcoplasmic reticulum. *Biophys. J.* **25**, 118*a*.

MATHIAS, R., LEVIS, R. & EISENBERG, R. (1980). Electrical models of excitation–contraction coupling and charge movement in skeletal muscle. *J. gen. Physiol.* **76**, 1–31.

RAKOWSKI, R. F. (1978*a*). Reprimed charge movement in skeletal muscle fibres. *J. Physiol.* **281**, 339–358.

RAKOWSKI, R. F. (1978*b*). Recovery of linear capacitance in skeletal muscle fibres. *Biophys. J.* **21**, 167*a*.

RAKOWSKI, R. F. (1978*c*). Immobilization of membrane charge in skeletal muscle fibres. *Physiologist* **21**, 95.

SCHNEIDER, M. F. (1970). Linear electrical properties of the transverse tubules and surface membrane of skeletal muscle fibers. *J. gen. Physiol.* **56**, 640–671.

SCHNEIDER, M. F. & CHANDLER, W. K. (1973). Voltage dependent charge movement in skeletal muscle: a possible step in excitation–contraction coupling. *Nature, Lond.* **242**, 224–226.

SCHNEIDER, M. F. & CHANDLER, W. K. (1976). Effects of membrane potential on the capacitance of skeletal muscle fibres. *J. gen. Physiol.* **67**, 125–163.